

ARTICLE

Differentiation of the binding of two ligands to a tetrameric protein with a single symmetric active site by ^{19}F NMR

Gabriel J. Fuente-Gómez | Creighton L. Kellum | Alexis C. Miranda |
Michael R. Duff Jr.  | Elizabeth E. Howell

Department of Biochemistry & Cellular and Molecular Biology, University of Tennessee-Knoxville, Knoxville, Tennessee

Correspondence

Michael R. Duff Jr., Department of Biochemistry & Cellular and Molecular Biology, University of Tennessee-Knoxville, Knoxville, Tennessee 37996.
Email: mduff5@utk.edu

Abstract

R67 dihydrofolate reductase (R67 DHFR) is a plasmid-encoded enzyme that confers resistance to the antibacterial drug trimethoprim. R67 DHFR is a tetramer with a single active site that is unusual as both cofactor and substrate are recognized by symmetry-related residues. Such promiscuity has limited our previous efforts to differentiate ligand binding by NMR. To address this problem, we incorporated fluorine at positions 4, 5, 6, or 7 of the indole rings of tryptophans 38 and 45 and characterized the spectra to determine which probe was optimal for studying ligand binding. Two resonances were observed for all apo proteins. Unexpectedly, the W45 resonance appeared broad, and truncation of the disordered N-termini resulted in the appearance of one sharp W45 resonance. These results are consistent with interaction of the N-terminus with W45. Binding of the cofactor broadened W38 for all fluorine probes, whereas substrate, dihydrofolate, binding resulted in the appearance of three new resonances for 4- and 5-fluoroindole labeled protein and severe line broadening for 6- and 7-fluoroindole R67 DHFR. W45 became slightly broader upon ligand binding. With only two peaks in the ^{19}F NMR spectra, our data were able to differentiate cofactor and substrate binding to the single, symmetric active site of R67 DHFR and yield binding affinities.

KEYWORDS

drug resistant enzyme, fluorine, NMR, protein NMR, R67 DHFR

Abbreviations and Symbols: 4F, 4-fluorotryptophan labeled; 5F, 5-fluorotryptophan labeled; 6F, 6-fluorotryptophan labeled; 7F, 7-fluorotryptophan labeled; δ_r , ring current effect on the chemical shift; DHF, dihydrofolate; DHFR, dihydrofolate reductase; HSQC, heteronuclear single quantum coherence spectroscopy; NADP⁺, oxidized form of nicotinamide adenine dinucleotide phosphate; R67 DHFR, R67-plasmid encoded DHFR

Statement: R67 dihydrofolate reductase is an antibiotic-resistant homotetramer with a single active site pore consisting of symmetry-related residues. Due to the symmetry in the active site, it is difficult to monitor ligand binding by conventional NMR techniques because of the complexity of spectra. ^{19}F NMR allowed us to differentiate binding of two ligands to the active site, and could potentially be used to screen for new inhibitors.

This is an open access article under the terms of the Creative Commons Attribution-NonCommercial-NoDerivs License, which permits use and distribution in any medium, provided the original work is properly cited, the use is non-commercial and no modifications or adaptations are made.

© 2020 The Authors. *Protein Science* published by Wiley Periodicals LLC. on behalf of The Protein Society.

1 | INTRODUCTION

R67 dihydrofolate reductase (DHFR) is a plasmid encoded enzyme that confers resistance to the extensively used antibiotic trimethoprim. This enzyme shares no sequence or structural homology with chromosomal DHFRs despite both enzymes catalyzing the same reaction.¹ R67 DHFR is a homotetramer with 222-symmetry and a single active site in a pore at the center of the structure (Figure 1(a)).² The same residues on each of the four monomers make up the active site surface, which results in binding sites on both sides of the pore that can bind either the substrate or the cofactor.³ Therefore, it is possible to form nonproductive complexes between two substrates or two cofactors as well as the productive complex with one substrate and one cofactor.⁴ Despite several decades of research on R67 DHFR, there are no drugs that target the enzyme, and only recently have inhibitors been designed that specifically target the enzyme.^{5,6}

Binding of the cofactor analog, NADP⁺, can be monitored by HSQC NMR; however, substrate, dihydrofolate (DHF), exhibits complex NMR spectra due to tighter binding of the ligand slowing the exchange kinetics and breaking up the protein symmetry, which increased the number of peaks.⁸ Therefore, a different NMR method is needed to study ligand and inhibitor binding to R67 DHFR. ¹⁹F NMR spectroscopy is sensitive enough to characterize protein-ligand interactions, and for drug discovery.^{9–13} ¹⁹F NMR can potentially overcome the problems of lost symmetry as it offers the advantage of being able to label select residues, which helps minimize

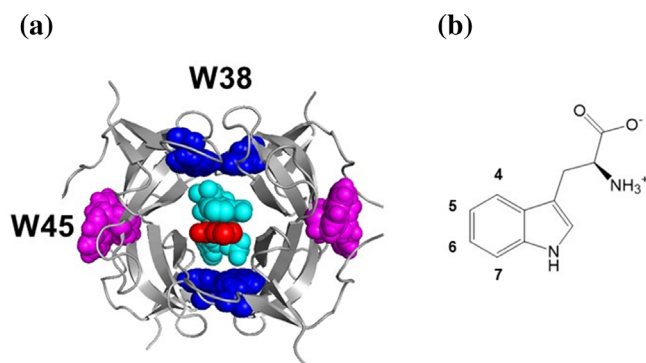


FIGURE 1 R67 DHFR is a homotetramer with two tryptophans per monomer. (a) W38 and its symmetry-related partners (blue) are located at the dimer-dimer interface of R67 DHFR (PDB ID: 2RK1),⁷ whereas the W45 residues (magenta) are located at the monomer-monomer interface. DHF (red) and NADP⁺ (cyan) bind in the pore formed in the center of the tetramer. The disordered N-termini are not present in the crystal structure. (b) The structure of tryptophan showing the numbering of the carbon atoms in the indole ring

the complexity of the spectra and the possibility of structural perturbations.^{14,15} Therefore, we labeled the tryptophans in R67 DHFR with fluorine and characterized ligand binding by ¹⁹F NMR. This approach could be used in the ongoing efforts to characterize binding of potential inhibitors to this drug resistant enzyme.

2 | RESULTS

2.1 | Assignment of ¹⁹F NMR peaks

Incorporation of probes with fluorine at four different positions in the tryptophan indole ring (Figure 1(b)) of R67 DHFR resulted in distinct NMR spectra in terms of chemical shifts and line width (Figure 2). Two peaks were observed for 4-, 5-, and 7-fluorine labeled proteins, a downfield sharp peak and an upfield broad one, however 6-fluorotryptophan (6F) R67 DHFR had two sharp peaks that flanked the broad band (Table S1). Fluorine incorporation into R67 DHFR was above 90% for all the four fluorotryptophans. The NMR assignment was achieved using the W45F mutant of R67 DHFR. Spectra for 4-fluorotryptophan (4F), 5-fluorotryptophan (5F), and 6F W45F R67 DHFR only contained the sharp peak, or two sharp peaks for 6F, while the broad peak was absent (Figure S1). Therefore, the sharp peaks that remained

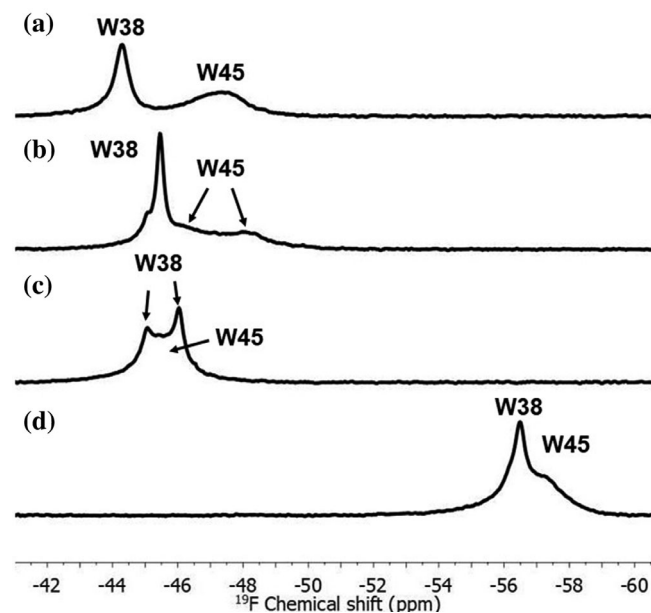


FIGURE 2 Fluorine incorporation in R67 DHFR exhibited characteristic NMR spectra for each position of the fluorine atom in the indole ring. Spectra are shown for (a) 4F R67 DHFR, (b) 5F R67 DHFR, (c) 6F R67 DHFR (W45 is underneath the W38 peak), and (d) 7F R67 DHFR

correspond to W38, whereas the broad peaks correspond to W45.

The 5F R67 DHFR spectrum contained a small shoulder corresponding to approximately 10% of the area of the sharp peak and two W38 peaks for 6F R67 DHFR (Figure 2). To determine if these additional W38 peaks arise from partial labeling of R67 DHFR, unlabeled protein was added, which increased the intensity of the downfield W38 peaks in both spectra (Figure S2). Tetramers with a mixture of labeled and unlabeled dimers were prepared by the pH-dependent dissociation of R67 DHFR from tetramers to dimers.^{16,17} The intensity of the downfield W38 peaks increased suggesting that the downfield peaks corresponded to partially labeled protein and the upfield peaks arose from fully labeled R67 DHFR.

Relative to W38, W45 exhibited severe line broadening. As slow exchange could be responsible for the broadening, spectra were acquired at higher temperatures (Figure S3); however, the W45 peak still remained broader than the W38 peak even at higher temperatures, which suggested broadening may arise from other reasons as well. The N-termini of R67 DHFR are disordered, forming a collapsed structure, interacting with themselves and the monomer-monomer interface of the tetramer core.^{2,18} Since W45 is located at the monomer-monomer interface, we hypothesized that the interaction of the disordered N-termini with W45 could be responsible for the broad peaks. The disordered N-termini can be cleaved by α -chymotrypsin from each of the protomers after Phe47 of R67 DHFR expressed from the pRSETb plasmid (Figure S4A), and the core of the enzyme remains intact and retains its activity.^{2,7,8,18–20} Truncation of 5F R67 DHFR sharpened both peaks (Figure S4). The chemical shift of W38 was unchanged by truncation. The N-termini do not interact with the dimer-dimer interface where W38 is located,¹⁸ and the absence or presence of the N-termini in the full-length versus truncated proteins were not expected to alter the chemical shift of W38. W45 sharpened significantly into a single peak with similar line width to the W38 peak, which indicated the N-termini induced the broadening of the W45 peaks.

2.2 | Titration of NADP⁺ and DHF to fluorinated R67 DHFRs

Whether ¹⁹F NMR could differentiate the binding of NADP⁺ from the substrate, DHF, was examined by NMR titrations. Binding of NADP⁺ to 4F and 6F R67 DHFR caused line broadening of the W38 peak with no change in the chemical shift, whereas the 5F and 7F R67 DHFR peaks shifted downfield in addition to broadening

(Figure 3, S5). Severe line broadening for the two W38 peaks in 6F R67 DHFR caused an overlap of the W45 peak, forming a broad envelope. W45 became slightly broader for all fluorine probes upon NADP⁺ binding.

Similar to the NADP⁺ titration, the W45 peaks broadened upon DHF titration into the fluorinated R67 DHFR-NADP⁺ binary complexes; however, W38 split into smaller peaks. Three new peaks appeared for 4F and 5F R67 DHFR (Figure 3). Increasing the temperature to 45°C sharpened both the W38 and W45 peaks of 4F R67 DHFR and resolved the resonances from the four symmetric W38 residues in the spectrum (Figure S6). In the 7F binary complex, W38 formed at least two peaks, with further line broadening (Figure S5D). In contrast to the other fluorine probes, DHF binding to the 6F R67 DHFR-NADP⁺ binary complex resulted in the appearance of seven new peaks with additional severe broadening (Figure S5C). Overall, our NMR titrations indicated that fluorine-labeled W38 could be used to differentiate binding of NADP⁺ from DHF.

We calculated the dissociation constants for NADP⁺ and DHF binding to R67 DHFR using either peak intensities or chemical shift changes as a function of ligand concentration (Table 1). The K_d s obtained for NADP⁺ were all within error (220–380 μ M), irrespective of the fluorine probe. These K_d s were 2–3 times higher than those reported previously by NMR and ITC, 132 μ M and 99 μ M, respectively.^{4,8} Most likely this discrepancy arises from the difference in the length of the disordered N-termini. Truncated R67 DHFR was used for previous NMR experiments, while the normal length R67 DHFR was used in ITC experiments. The longer N-terminus of the pRSETb his-tag construct, with a molecular weight of 47 kDa, also increased the K_m s of NADPH and DHF two-fold compared to the 33 kDa normal length R67 DHFR.²¹ DHF binding to the 4F, 5F, and 7F R67 DHFRs yielded K_d s within error of each other; however, when 6-fluoroindole was used as the probe, the K_d could not be accurately determined as it had an error of 100%. These values were also 6 to 8 times higher than ITC, 4.8 ± 1.0 μ M, R67 DHFR with normal length N-termini.^{4,8}

3 | DISCUSSION

The presence of only two tryptophan peaks in the spectra of apo R67 DHFR is consistent with the 222-symmetry of the homotetrameric protein, where each symmetry-related W38 (or W45) residue samples a similar environment.² Therefore, the chemical shifts of all four symmetry-related tryptophan residues were either the same or significantly overlapping. Single peaks for W38

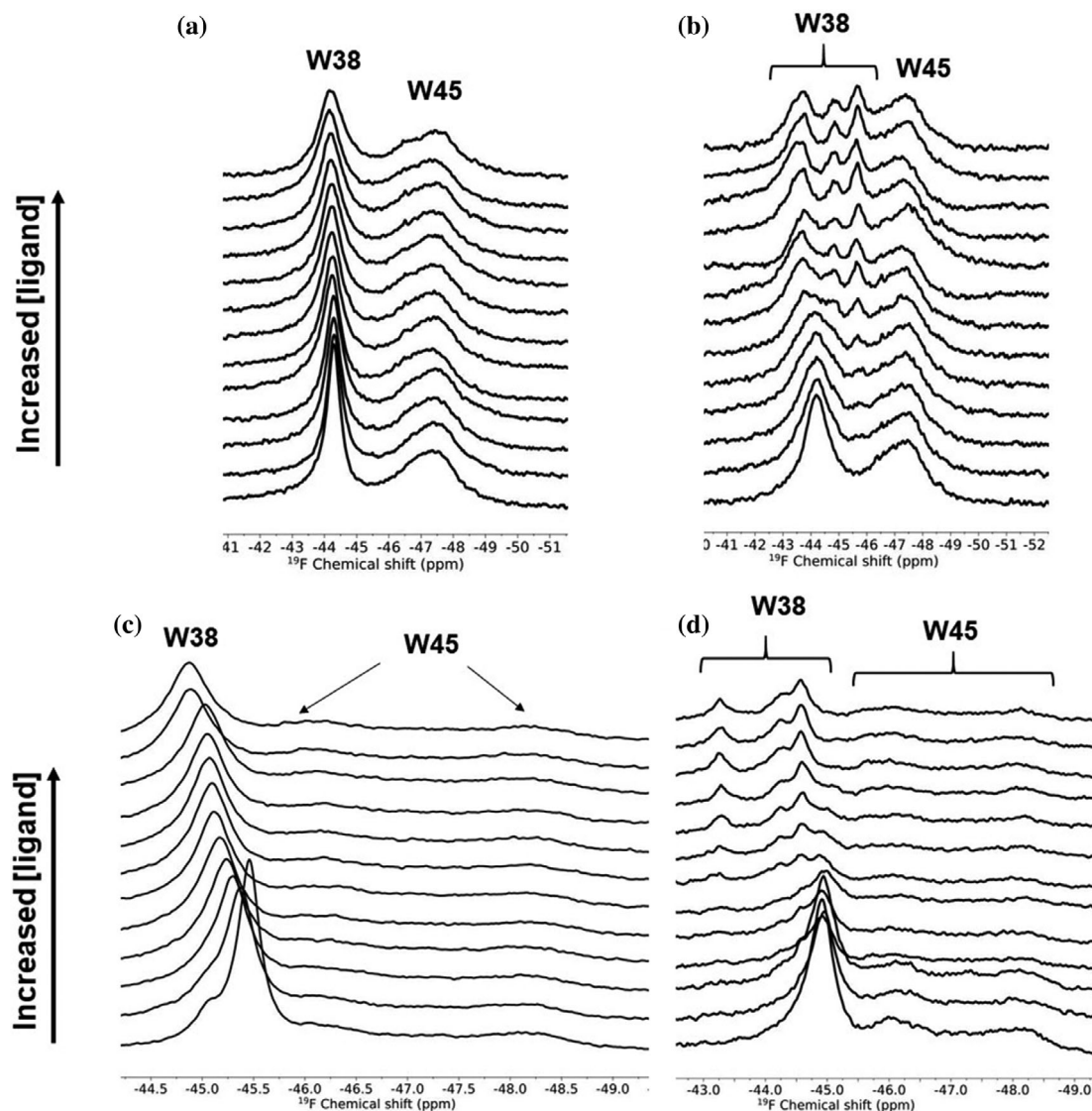


FIGURE 3 ^{19}F NMR spectra for the titration of 4F and 5F R67 DHFR with ligands. Titration of (a) 0, 0.15, 0.30, 0.44, 0.59, 0.87, 1.2, 1.4, 1.9, 2.4, 4.0, 8.0 and 14.5 mM NADP^+ into 4F R67 DHFR, (b) 0, 0.05, 0.10, 0.15, 0.20, 0.38, 0.43, 0.48, 0.75, 1.5, 3.6 and 5.0 mM DHF into 4F R67 DHFR saturated with 6 mM NADP^+ , (c) 0, 0.27, 0.54, 0.81, 1.1, 1.3, 1.6, 1.8, 2.1, 2.4, 9.1, 14.4 mM NADP^+ to 5F R67 DHFR, and (d) 0, 0.04, 0.09, 0.13, 0.15, 0.22, 0.30, 0.50, 0.60, 0.70, 1.0, 1.8, 4.5 mM DHF into 5F R67 DHFR saturated with 6 mM NADP^+

TABLE 1 Dissociation constants of R67 DHFR obtained by NMR

Enzyme	K_d (μM) ^a	
	NADP^+	DHF
Truncated WT	132 ± 51^b	ND ^c
4F R67 DHFR	360 ± 66	42 ± 13
5F R67 DHFR	220 ± 20^d	33 ± 20
6F R67 DHFR	320 ± 70	110 ± 120
7F R67 DHFR	380 ± 60	30 ± 28

^a K_d s were obtained using peak intensity.

^bdata were obtained from Reference⁸.

^cNot determined.

^d K_d obtained by measuring chemical shift.

and W45 are consistent with the HSQC NMR data that yield single peaks for each residue due to the symmetry of R67 DHFR.⁸ For 4F, 5F, and 7F R67 DHFR, W38 is downfield of the W45 peak, which is consistent with W38 being buried in a hydrophobic environment at the dimer-dimer interface and W45 being exposed to solvent at the monomer-monomer interface (Figure 1(a)).^{7,22} A sharp peak for W38 is consistent with the presence of single conformations in the crystal structure.

The broad W45 bands were consistent with neutron scattering data that suggested that the disordered N-termini collapse and interact with the monomer-monomer interface where W45 is located.¹⁸ Indeed, truncation of the disordered N-termini resulted in the

sharpening of W45 in 5F R67 DHFR (Figure S4). W45 populates two conformations in the crystal structure (Figure S7).⁷ A single peak for W45 in the truncated 5F R67 DHFR indicates that either the exchange between these two conformations is fast on the time scale of the NMR experiment, or that there is not a significant difference in the environment between the two conformations.

3.1 | Changes in the ¹⁹F NMR spectra of R67 DHFR upon ligand binding

All four fluorine probes were able to differentiate between NADP⁺ and DHF binding. Binding of the cofactor analog, NADP⁺, to all fluorinated proteins resulted in the broadening of both W38 and W45 (Figure 3, S5). HSQC experiments yielded similar results where both W38 and W45 shifted upon addition of NADP⁺ due to changes in hydrogen bonding between the β -sheets in the bound complex.⁸ However, the factors that caused a 0.4 ppm change in the chemical shift for W45 in the HSQC spectra, caused only slight broadening in the ¹⁹F NMR that could not be used to quantify binding. Slight broadening of W45 upon NADP⁺ binding is consistent with the distance of the residue from the active site and the lower sensitivity of W45 fluorescence, relative to W38, to NADPH binding.¹⁷ Broadening of W38 upon NADP⁺ binding, on the other hand, may arise either due to fast ligand association/dissociation rates with the protein, a slow conformational change, or dephosphorylation, of NADP⁺ bound to R67 DHFR,⁸ or from the vicinity of W38 to the active site. While W38 does not interact with the bound ligands directly, the residue is positioned adjacent to a hydrogen bond network formed between Q67 and Y69 that are in direct contact with the bound ligand, and becomes more compact upon cofactor binding.⁷

Upon DHF binding, W38 splits into multiple smaller peaks (Figure 3, S5). The upfield-most W38 peak in 4F R67 DHFR, or the downfield most peak in 5F R67 DHFR, had twice the area of the other two smaller peaks. The W38 peaks overlapped in 6F and 7F R67 DHFR due to splitting and line broadening making it difficult to determine if one of the peaks had twice the area of the others. Some of the broadening in the spectra may be due to a slow conformational change, or dephosphorylation of NADP⁺ that occurs in the ternary complex.⁸ DHF binding to the R67 DHFR-NADP⁺ complex is much tighter than cofactor binding to the apo protein due to cooperativity.⁴ Tighter association in the ternary complex potentially splits the peaks because of the decreased association/dissociation rates and the breaking of the

symmetry of the protein as the two halves of the active site pore have different ligands bound. Loss of peak degeneracy in the ternary complex similarly occurred in previous HSQC experiments, which made the spectra more complex.⁸ However, labeling of the two tryptophan residues with fluorine yielded two ¹⁹F NMR peaks in the binary complex, and four in the ternary complex, which simplified distinguishing cofactor and substrate binding and measuring ligand affinity compared to HSQC. Ring current shifts from the proximity of the one aromatic pterin ring of DHF to W38 could also play a role in splitting of the peak. Shifts around 1 ppm are typically noted from ring current effects in ¹⁹F NMR.²³ Calculations of DHF ring current shifts (δ_r) on the four W38 residues labeled with fluorine were performed in MatLab (v. 2019b) according to Johnson and Bovey,²⁴ and yielded δ_r s between -0.12 and 0.28 (Table S2). Most of the new W38 peaks noted upon DHF binding shifted by at least ± 0.5 ppm from the binary complex peak (Table S1), indicating that ring current shifts from DHF could only account for some of the W38 peak splitting in the ternary complex. A third potential reason for splitting of the W38 peak upon DHF binding could be due to motion of the glutamate tail of the substrate. Crystal structure and molecular dynamics simulation data indicated that the tail of the substrate is dynamic.^{7,25,26} Two symmetry-related lysines 32s at the top of one side of the pore constrain the position of NADP⁺ by forming ionic interactions with the phosphate groups.⁷ In the other half of the pore, the glutamate tail of DHF is not well resolved in the crystal structure and switches between forming direct ion pairs with the K32s on that side of the pore.^{25–27} This could result in two different environments for the W38 residues on the side of the pore with bound DHF, one where the glutamate tail is nearby, and the other where the glutamate tail is further away.

3.2 | Quantifying ligand binding affinity

Binding affinities for NADP⁺ obtained from our NMR titrations with the four different fluorindole probes were within error, indicating that all four probes are adequate to study cofactor binding. However, ¹⁹F NMR could not accurately measure substrate binding as the K_d s were 5- to seven-fold higher than previously reported for R67 DHFR.⁴ The protein concentration used in our ¹⁹F NMR experiments most likely accounts for the poor estimate of the K_d s. Optimal protein concentrations for estimating binding affinity should be less than half of the K_d .²⁸ However, in our DHF experiments, the protein concentrations were about 40-fold higher than the K_d , and thus do not give accurate estimates of the binding affinity. Lowering

our R67 DHFR concentrations below 0.2 mM could potentially have improved our analysis of the K_d . However, the pRSETb R67 DHFR construct has a molecular weight of 47 kDa, and broad ^{19}F peaks that hinder using lower protein concentrations in NMR. Additionally, decomposition of DHF after several hours prohibited longer scan times that would result from increasing the number of scans to improve the signal-to-noise.

3.3 | Optimal fluorine probe for R67 DHFR

While each fluorine probe exhibited line broadening upon NADP^+ binding, the 4F and 5F had larger chemical shift dispersions and well-resolved W38 and W45 peaks. Others have reported that 5-fluorotryptophan yields greater chemical shift dispersion²⁹ or better resolution³⁰ over 4- and 6-tryptophan probes. Overlap and broadening of the 6F and 7F R67 DHFR peaks upon ligand binding led to 100% errors in the substrate K_d s, which indicates that poor resolution with these fluorine probes may hinder measuring ligand binding to R67 DHFR. In summary, ^{19}F NMR can differentiate binding of NADP^+ and DHF to symmetry-related residues in the active site of R67 DHFR, and could be used for potential exploration of inhibitors of this antibiotic-resistant enzyme.

4 | MATERIALS AND METHODS

4.1 | Expression and purification of ^{19}F -labeled R67 DHFR

Fluorine-labeled tryptophans were incorporated as described by Crowley et al.³¹ To facilitate protein purification, a his-tagged construct of R67 DHFR cloned into a pRSETb vector, which has an additional 30 residues added to the disordered N-terminus compared to the normal length R67 DHFR,²¹ was used. A W45F mutant was prepared as described.¹⁷ Cells were grown in rich media at 37°C to an O.D. 600 of 0.6. The cells were harvested by centrifugation and the pellet was resuspended in an equal volume of pre-warmed minimal medium (7.5 mM $[\text{NH}_4]_2\text{SO}_4$, 50 mM Na_2HPO_4 and 50 mM KH_2PO_4 pH 7.0). 4-, 5-, 6- or 7-Fluoroindoles were dissolved in dimethyl sulfoxide and added to the media (final concentration of 60 mg/L). After 30 minutes of acclimatization, protein expression was induced with the addition of 1 mM IPTG for 10 h. Protein was purified on a nickel-NTA column (Qiagen).⁸ Purified protein was dialyzed against deionized H_2O , lyophilized, and stored at 4°C.

α -Chymotrypsin-truncated R67 DHFR was prepared as described.^{18,19} Protein concentrations were determined by measuring the absorbance at 280 nm using extinction coefficients (1.15, 1.38, 1.35, and 1.19 ml/mg for 4F, 5F, 6F, and 7F R67 DHFR, respectively) determined with a bicinchoninic acid assay (Pierce).

4.2 | NMR experiments

Lyophilized R67 DHFR (100–750 μM tetramer) was dissolved in 10 mM perdeuterated Tris-DCI (Tris-d11) buffer, pH 8.0 in D_2O . ^{19}F NMR measurements were acquired on a Varian 500 MHz spectrophotometer equipped with a OneNMR probe operating at 470 MHz. ^{19}F spectra were obtained with 512 scans, a spectral width of 230 ppm, relaxation delay of 1 second, and 87° pulse angle. The ^{19}F chemical shifts were referenced to 10 mM trifluoroacetic acid. All NMR data were processed using MestReNova (Mestrelab) applying a 20 Hz line-broadening. Fluorine incorporation levels were measured by integrating the area of a known concentration of labeled apo R67 DHFR and comparing to an internal 10 mM trifluoroacetic acid standard.

Incomplete labeling of 5F and 6F R67 DHFR was explored using the pH-induced tetramer-to-dimer dissociation of R67 DHFR.¹⁶ The NMR spectra for 5F or 6F R67 DHFR were obtained at pH 8. Next, the fluorine-labeled R67 DHFR was mixed with a molar equivalent of unlabeled R67 DHFR, equilibrated for 5 min. Subsequently, the pH of the mixture of labeled and unlabeled R67 DHFR was lowered to pH 5 to form dimeric R67 DHFR. Finally, the pH of the solution was adjusted back to pH 8 to reform the tetramer, which should be a mixture of fully labeled, fully unlabeled, and partially labeled R67 DHFR tetramers. NMR spectra were recorded at each step.

4.3 | Ligand binding studies by ^{19}F NMR

NMR titrations were performed at 25°C by titrating 0.6–1 mM labeled R67 DHFR with increasing concentrations (0–20 mM) of NADP^+ . Binding data for the ternary complex were obtained by titrating DHF (0–3.5 mM) into a binary complex of R67 DHFR (0.17–1 mM) saturated with 6 mM NADP^+ . Ligand concentrations were measured using their respective extinction coefficients, 28,000 $\text{M}^{-1} \text{cm}^{-1}$ at 282 nm for DHF and 18,000 $\text{M}^{-1} \text{cm}^{-1}$ at 259 nm for NADP^+ . Both binding of NADP^+ to apo R67 DHFR and DHF to the R67 DHFR- NADP^+ binary complex have stoichiometries of one and were fit to a 1:1 binding model.⁴ Dissociation constants

were calculated by plotting either changes in chemical shifts (for NADP⁺ binding to 5F R67 DHFR) or peak intensities (for 4F, 6F, and 7F R67 DHFR and DHF binding to 5F R67 DHFR) as a function of ligand concentration and fitting the curve to Equation 1²⁸:

$$\frac{LP}{P} = \frac{-(K_d + L + P) \pm \sqrt{(K_d + L + P)^2 - 4B}}{2P} \quad (1)$$

where K_d is the dissociation constant of the ligand, L is the total ligand concentration, P is the total protein concentration, and B is $L \cdot P$. The data were fit using Sigma Plot 12. Similar K_d s were obtained for DHF binding whether loss of the binary peak, or increase in the ternary peaks, was measured.

ACKNOWLEDGEMENTS

The authors would like to dedicate this article to the memory of Dr. Liz Howell who unfortunately passed away on April 9, 2019. We would also like to thank Dr. Engin Serpersu (UTK) for helpful discussion of this work and Drs. Gladys Alexandre, Daniel Roberts, and Francisco Barrera (UTK) for critical reading of the manuscript. Funding was from NIH (grant GM 110669) to EEH and The University of Tennessee Summer Graduate Research Assistantship Fund to GJFG in 2019.

The authors declare no conflict of interest.

AUTHOR CONTRIBUTIONS

Gabriel Fuente-Gomez: Data curation; formal analysis; investigation; writing-original draft; writing-review and editing. **Creighton Kellum:** Investigation. **Alexis Miranda:** Investigation. **Michael Duff:** Data curation; formal analysis; supervision; writing-original draft; writing-review and editing. **Elizabeth Howell:** Conceptualization; funding acquisition; resources; supervision.

REFERENCES

- Howell EE. Searching sequence space: Two different approaches to dihydrofolate reductase catalysis. *ChemBiochem*. 2005;6:590–600.
- Narayana N, Matthews DA, Howell EE, Nguyen-huu X. A plasmid-encoded dihydrofolate reductase from trimethoprim-resistant bacteria has a novel D2-symmetric active site. *Nat Struct Biol*. 1995;2:1018–1025.
- Strader MB, Smiley RD, Stinnett LG, VerBerkmoes NC, Howell EE. Role of S65, Q67, I68, and Y69 residues in homotetrameric R67 dihydrofolate reductase. *Biochemistry*. 2001;40:11344–11352.
- Bradrick TD, Beechem JM, Howell EE. Unusual binding stoichiometries and cooperativity are observed during binary and ternary complex formation in the single active pore of R67 dihydrofolate reductase, a D2 symmetric protein. *Biochemistry*. 1996;35:11414–11424.
- Toulouse JL, Yachnin BJ, Ruediger EH, et al. Structure-based design of dimeric bisbenzimidazole inhibitors to an emergent trimethoprim-resistant type II dihydrofolate reductase guides the design of monomeric analogues. *ACS Omega*. 2019;4:10056–10069.
- Bastien D, Ebert MC, Forge D, et al. Fragment-based design of symmetrical bis-benzimidazoles as selective inhibitors of the trimethoprim-resistant, type II R67 dihydrofolate reductase. *J Med Chem*. 2012;55:3182–3192.
- Krahn JM, Jackson MR, DeRose EF, Howell EE, London RE. Crystal structure of a type II dihydrofolate reductase catalytic ternary complex. *Biochemistry*. 2007;46:14878–14888.
- Pitcher WH 3rd, DeRose EF, Mueller GA, Howell EE, London RE. NMR studies of the interaction of a type II dihydrofolate reductase with pyridine nucleotides reveal unexpected phosphatase and reductase activity. *Biochemistry*. 2003;42:11150–11160.
- Sharaf NG, Xi Z, Ishima R, Gronenborn AM. The HIV-1 p66 homodimeric RT exhibits different conformations in the binding-competent and -incompetent NNRTI site. *Proteins*. 2017;85:2191–2197.
- Ye L, Van Eps N, Zimmer M, Ernst OP, Prosser RS. Activation of the A2A adenosine G-protein-coupled receptor by conformational selection. *Nature*. 2016;533:265–268.
- Evanics F, Kitevski JL, Bezsonova I, Forman-Kay J, Prosser RS. ¹⁹F NMR studies of solvent exposure and peptide binding to an SH3 domain. *Biochim Biophys Acta*. 2007;1770:221–230.
- Richards KL, Rowe ML, Hudson PB, Williamson RA, Howard MJ. Combined ligand-observe (19)F and protein-observe (15)N,(1)H-HSQC NMR suggests phenylalanine as the key delta-somatostatin residue recognized by human protein disulfide isomerase. *Sci Rep*. 2016;6:1–9.
- Pomerantz WC, Wang N, Lipinski AK, Wang R, Cierpicki T, Mapp AK. Profiling the dynamic interfaces of fluorinated transcription complexes for ligand discovery and characterization. *ACS Chem Biol*. 2012;7:1345–1350.
- Arntson KE, Pomerantz WC. Protein-observed fluorine NMR: A bioorthogonal approach for small molecule discovery. *J Med Chem*. 2016;59:5158–5171.
- Sharaf NG, Gronenborn AM. ¹⁹F-modified proteins and ¹⁹F-containing ligands as tools in solution NMR studies of protein interactions. *Methods Enzymol*. 2015;565:67–95.
- Nichols R, Weaver CD, Eisenstein E, et al. Titration of histidine 62 in R67 dihydrofolate reductase is linked to a tetramer <-> two-dimer equilibrium. *Biochemistry*. 1993;32:1695–1706.
- West FW, Seo HS, Bradrick TD, Howell EE. Effects of single-tryptophan mutations on R67 dihydrofolate reductase. *Biochemistry*. 2000;39:3678–3689.
- Bhojane PP, Duff MR Jr, Bafna K, Agarwal P, Stanley C, Howell EE. Small angle neutron scattering studies of R67 dihydrofolate reductase, a tetrameric protein with intrinsically disordered N-termini. *Biochemistry*. 2017;56:5886–5899.
- Reece LJ, Nichols R, Ogden RC, Howell EE. Construction of a synthetic gene for an R-plasmid-encoded dihydrofolate reductase and studies on the role of the N-terminus in the protein. *Biochemistry*. 1991;30:10895–10904.

20. Yachnin BJ, Colin DY, Volpato JP, Ebert M, Pelletier JN, Berghuis AM. Novel crystallization conditions for tandem variant R67 DHFR yield a wild-type crystal structure. *Acta Cryst D*. 2011;67:1316–1322.
21. Strader, MB. Constructing a hybrid of R67 dihydrofolate reductase to study asymmetric mutations in the active site. MS thesis, Department of Biochemistry & Cellular and Molecular Biology University of Tennessee, Knoxville, TN; 1998.
22. Dalvit C, Vulpetti A. Fluorine-protein interactions and ^{19}F NMR isotropic chemical shifts: An empirical correlation with implications for drug design. *ChemMedChem*. 2011;6:104–114.
23. Lau EY, Gerig JT. Origins of fluorine NMR chemical shifts in fluorine-containing proteins. *J Am Chem Soc*. 2000;122:4408–4417.
24. Johnson CE, Bovey FA. Calculation of nuclear magnetic resonance spectra of aromatic hydrocarbons. *J Chem Phys*. 1958;29:1012–1014.
25. Kamath G, Howell EE, Agarwal PK. The tail wagging the dog: Insights into catalysis in R67 dihydrofolate reductase. *Biochemistry*. 2010;49:9078–9088.
26. Alonso H, Gillies MB, Cummins PL, Bliznyuk AA, Gready JE. Multiple ligand-binding modes in bacterial R67 dihydrofolate reductase. *J Comput Aided Mol Des*. 2005;19:165–187.
27. Hicks SN, Smiley RD, Hamilton JB, Howell EE. Role of ionic interactions in ligand binding and catalysis of R67 dihydrofolate reductase. *Biochemistry*. 2003;42:10569–10578.
28. Williamson MP. Using chemical shift perturbation to characterise ligand binding. *Prog Nucl Magn Reson Spectrosc*. 2013;73:1–16.
29. Luck LA, Falke JJ. ^{19}F NMR studies of the D-galactose chemosensory receptor. 1. Sugar binding yields a global structural change. *Biochemistry*. 1991;30:4248–4256.
30. Ho C, Pratt EA, Rule GS. Membrane-bound D-lactate dehydrogenase of *Escherichia coli*: A model for protein interactions in membranes. *Biochim Biophys Acta*. 1989;988:173–184.
31. Crowley PB, Kyne C, Monteith WB. Simple and inexpensive incorporation of ^{19}F -tryptophan for protein NMR spectroscopy. *Chem Commun*. 2012;48:10681–10683.

ORCID

Michael R. Duff Jr  <https://orcid.org/0000-0002-8581-7102>

SUPPORTING INFORMATION

Additional supporting information may be found online in the Supporting Information section at the end of this article.

How to cite this article: Fuente-Gómez GJ, Kellum CL, Miranda AC, Duff MR Jr, Howell EE. Differentiation of the binding of two ligands to a tetrameric protein with a single symmetric active site by ^{19}F NMR. *Protein Science*. 2021;30:477–484. <https://doi.org/10.1002/pro.4007>